Actinomycin D–Deoxynucleotide Complexes as Models for the Actinomycin D–DNA Complex. The Use of Nuclear Magnetic Resonance to Determine the Stoichiometry and the Geometry of the Complexes†

Thomas R. Krugh* and Yu-Chih Chen

ABSTRACT: The use of proton and carbon-13 magnetic resonance spectroscopy for the determination of the geometry and the stoichiometry of the actinomycin D–deoxyguanosine 5′-monophosphate complex is outlined. The dimerization of actinomycin D has been reexamined by recording the proton magnetic resonance spectrum of actinomycin D to much lower concentrations through the use of Fourier transform nuclear magnetic resonance techniques. The effect of the actinomycin D dimerization on the observed chemical shifts that results from the addition of nucleotides to an actinomycin D solution is directly demonstrated by comparing the actinomycin D–nucleotide titrations at both low (~0.3 m*M*) and high (~12 m*M*) concentrations of actinomycin D. In the presence of excess nucleotide the chemical shifts of the actinomycin D groups were essentially the same for both the low and high concentration titrations. The complexes of actinomycin D with pdG-dC, dG-dC, deoxyguanosine 3′-monophosphate, G-C, C-G, dIMP(5′), 2,6-diaminopurine deoxyribose, and other nucleotides were also investigated by proton magnetic resonance and visible spectral titrations. These data were interpreted in terms of the molecular geometry of the complexes and in terms of the effect of the structure of the nucleotide base on the relative binding affinity of the nucleotides for the two nucleotide binding sites of actinomycin D. The carbon-13 chemical shifts of dGMP(5′) were measured as a function of concentration over the concentration range of 0.5–0.025 *M*. The infinite dilution carbon-13 chemical shifts were graphically estimated from the dilution curves. These values were used to calculate the changes in the chemical shifts of the dGMP carbons that result from the formation of an actinomycin D–$(dGMP)_2$ complex. It was not possible to interpret these carbon-13 chemical shift changes in terms of only ring current effects, which thus rules out the use of carbon-13 spectroscopy in the determination of the geometries of the actinomycin D complexes with the mono- and dinucleotides. The induced chemical shifts in the proton spectra may be used in the determination of the geometries of the complexes. A consideration of these data for the above nucleotide series shows that the predominant complex formed is one in which the guanine rings in the two nucleotide binding sites of actinomycin D are oriented in a manner very similar to that observed in the cocrystalline complex of actinomycin D with deoxyguanosine.

Actinomycin D binds to double-stranded DNA and effectively inhibits RNA synthesis (Kirk, 1960; Kersten et al. 1960; Kersten, 1961). The interaction of actinomycin D (Figure 1) with DNA has been studied by a variety of techniques (for reviews see Reich and Goldberg, 1965; Goldberg and Friedman, 1971; Sobell, 1973). When actinomycin D binds to DNA there is a general requirement for the presence of a guanine base, an observation that led Sobell and coworkers (Sobell et al., 1971; Jain and Sobell, 1972; Sobell and Jain, 1972) to cocrystallize actinomycin D with deoxyguanosine. The structure of this cocrystalline complex provided an excellent basis for proposing a model for the actinomycin D–DNA complex (Sobell and Jain, 1972; Sobell, 1973). We have investigated the interaction of actinomycin D with deoxydinucleotides and deoxymononucleotides as models for the actinomycin D–DNA complex (Krugh, 1972, 1974; Krugh and Neely, 1973a,b) and have shown that actinomycin D has a remarkable ability to recognize and preferentially orient the nucleotide bases. These studies also showed that the dinucleotides serve as excellent model systems for studying drug–nucleic acid complexes, an observation that has been confirmed by our studies on ethidium bromide (Krugh, 1974; Krugh et al., 1975b) which show that ethidium bromide will also selectively bind to the deoxydinucleotides and ribodinucleoside monophosphates to form an intercalated miniature double helical complex in aqueous solution. Knowing our preliminary results (Krugh et al., 1975), Sobell and coworkers easily cocrystallized ethidium bromide with ribodinucleoside monophosphates and have obtained a beautiful X-ray crystallographic visualization of drug–nucleic acid intercalative binding (Tsai et al., 1975). Additional support for the use of the dinucleotides as nucleic acid models comes from experiments which have shown that the deoxydinucleotides (Krugh and Young, 1975; Young and Krugh, 1975) and ribodinucleoside monophosphates (Krugh and Laing, unpublished results) self-associate in aqueous solution to form double helical complexes.

In this manuscript we reexamine the actinomycin D dimerization and the effect of aggregation upon the interpretation of proton and carbon-13 induced chemical shifts in terms of a geometry of the complex. The data support our previous conclusions (Krugh and Neely, 1973a,b) that actinomycin D forms a complex with *two* guanine containing nucleotides (such as 5′-dGMP and pdG-dC) in which the guanine rings are oriented with respect to the phenoxazone ring of actinomycin D in a manner similar to that observed

† From the Department of Chemistry, University of Rochester, Rochester, New York 14627. *Received April 22, 1975.* This investigation was supported by Public Health Service Research Grant No. CA-14103 from the National Cancer Institute.

in the cocrystalline complex of actinomycin D with deoxyguanosine. The complex formation of actinomycin D with deoxyinosine 5′-monophosphate, 2,6-diaminopurine deoxyribose, G-C, and C-G are also investigated and interpreted in terms of the geometry of the complexes formed and the relative preference of the nucleotides for binding to the two nucleotide binding sites of actinomycin D.

Experimental Section

Actinomycin D(Act D)[1] was a gift of Merck Sharp and Dohme. The samples of actinomycin D were either dissolved in D_2O and lyophilized, or were placed under vacuum for 1 hr before use, in order to remove a small amount of the crystallizing solvent. The deoxydinucleotides were purchased from Collaborative Research, the ribonucleotides were purchased from either Sigma or P-L Biochemicals. The mononucleotides were used without additional purification while the dinucleotides were passed through a Millipore filter after dissolution in a 5 m*M*, pH 7.0, phosphate buffer. The concentrations of all solutions were determined spectrophotometrically. The value of ϵ_{425} 23,500 (Smith, 1963) was used for actinomycin D. The extinction coefficients listed in P-L Biochemicals catalog no. 103 for the deoxydinucleoside monophosphates and ribodinucleoside monophosphates were used for all the dinucleotides. The presence of the terminal phosphate in the deoxydinucleotides is not expected to significantly change the magnitude of the extinction coefficient of λ_{max} for the respective deoxydinucleoside monophosphate since it does not affect the location of λ_{max}.

The nuclear magnetic resonance spectra (NMR) (^1H and ^{13}C) were recorded on a JEOL PFT-100 with an EC-100 computer. A 180°-τ-90° (WEFT) pulse sequence was used to minimize the residual water magnetization (Patt and Sykes, 1972; Benz et al., 1972; Mooberry and Krugh, 1975). For the proton magnetic resonance (^1H NMR) titrations the spectrum of the stock actinomycin D solution was measured, then small amounts of a concentrated nucleotide solution were added and the spectrum was recorded between each addition. The temperature was determined from the chemical shift of a methanol sample, using the calibration data of Van Geet (1970). The proton chemical shifts are given with respect to sodium 3-trimethylsilylpropionate-*2,2,3,3-d*$_4$ (Merck) which was used as an internal reference. The reference compound did not influence the chemical shifts of the actinomycin D or nucleotide resonances. The carbon-13 chemical shifts were measured relative to dioxane and then converted to a tetramethylsilane reference using 126.3 ppm as the downfield chemical shift of dioxane with respect to Me_4Si (Levy and Cargioli, 1972). The deoxyguanosine 5′-monophosphate (5′-dGMP) used in the ^{13}C studies was passed through a Chelex-100 (Bio-Rad) column to remove any paramagnetic impurities. This procedure, or the addition of a trace amount of EDTA, was also used for the other nucleotides if a significant line broadening was observed in the spectrum of the nucleotide. The assignment of the ^1H NMR spectrum of actinomycin D in D_2O has been previously reported (Arison and Hoogsteen, 1970; Angerman et al., 1972) and these assignments were used.

Aliquots of the actinomycin D solution (1.5–2.0 ml) were used for the visible spectral titrations. The nucleotides were added with a Hamilton microliter syringe through a preequilibrated rubber septum on the top of a 1-cm cell. The spectra were corrected for the dilution effect of the nucleotide additions by using the equation

$$\Delta A = A_{obsd}\left(\frac{\text{total volume}}{\text{original volume}}\right) - A_{original} \qquad (1)$$

where A_{obsd} is the observed absorbance for a particular solution and $A_{original}$ is the absorbance of the original actinomycin D solution at the start of the titration. An equivalent volume of deoxydinucleotide was added to a reference cell containing buffer solution if the deoxydinucleotide stock solution was not clear to the eye after filtering. The experiments utilizing the method of continuous variation (Job, 1928) were performed at 3°C in a 2-mm cell. The concentrations of actinomycin D and the dinucleotide were varied so that each solution had a total concentration (actinomycin D + dinucleotide) of 4×10^{-4} *M*.

All samples were dissolved in a 5 m*M*, pH_{meter} 7.0, phosphate buffer solution, with the exception of the 5′-dGMP samples used for the ^{13}C studies, in which no buffer was used but the pH was checked and adjusted (if necessary) after each dilution.

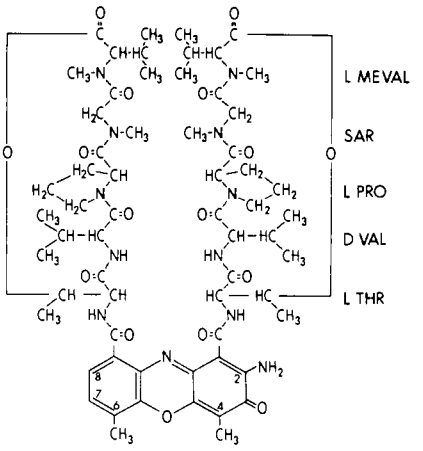

FIGURE 1: Structural formula of actinomycin D. Abbreviations used are: Thr, threonine; Val, valine; Pro, proline; Sar, sarcosine; MeVal, methylvaline.

Results

Actinomycin D Dimerization. In order to determine the changes in the chemical shifts that result from the formation of an actinomycin D–nucleotide complex it is important that the infinite dilution chemical shifts be measured for both the actinomycin D molecule and the nucleotide of interest since both actinomycin D and the nucleotides self-associate in aqueous solutions. Ultracentrifugation studies have shown that actinomycin D self-associates by the formation of dimers (Crothers et al., 1968). Proton magnetic resonance studies have shown that the actinomycin D dimer is formed by a vertical stacking of the phenoxazone rings with one ring inverted with respect to the other (Angerman et al., 1972; Krugh and Neely, 1973a). We have reexamined the concentration dependence of the actinomycin D resonances using pulsed Fourier transform NMR techniques which have allowed us to record the proton spectrum of actinomycin D at a much lower concentration than was previously possible (Figure 3). Note that when the actinomycin D dimer is formed the 4-CH_3 resonance is shifted upfield much more than either the 6-CH_3 or H(7) and H(8)

[1] Abbreviations used are: Act D, actinomycin D; 2,6-DAPDR, 2,6-diaminopurine deoxyribose.

Table I: Actinomycin D Dimerization Parameters.

Temp, (°C)		0.2 M NaCl[a]				No Salt[a]		
		δ_A (ppm)	δ_{A_2} (ppm)	$K_d \times 10^{-3} M^{-1}$		δ_A (ppm)	δ_{A_2} (ppm)	$K_d \times 10^{-3} M^{-1}$
6	4-CH_3	2.29 ± 0.03	1.55 ± 0.01	2.1 ± 0.3	4-CH_3	2.26 ± 0.04	1.55 ± 0.01	1.7 ± 0.3
	6-CH_3	2.67 ± 0.02	2.45 ± 0.01	(2.1 ± 0.3)[b]	6-CH_3	2.65 ± 0.02	2.46 ± 0.01	(1.7 ± 0.3)[b]
	H(7), H(8)	7.53 ± 0.01	7.44 ± 0.01	(2.1 ± 0.3)[b]	H(7), H(8)	7.52 ± 0.01	7.44 ± 0.01	(1.7 ± 0.3)[b]
25	4-CH_3	2.29 ± 0.02	1.66 ± 0.02	1.1 ± 0.2	4-CH_3	2.28 ± 0.02	1.64 ± 0.02	1.0 ± 0.2
	6-CH_3	2.63 ± 0.02	2.36 ± 0.01	(1.1 ± 0.2)[b]	6-CH_3	2.63 ± 0.02	2.38 ± 0.01	(1.0 ± 0.2)[b]
	H(7), H(8)	7.51 ± 0.02	7.43 ± 0.02	(1.1 ± 0.2)[b]	H(7), H(8)	7.52 ± 0.01	7.40 ± 0.01	(1.0 ± 0.2)[b]

[a] All samples were dissolved in a 5 mM, pH_{meter} 7.0, phosphate buffer in D_2O. [b] The values of δ_A and δ_{A_2} for the 6-CH_3 and H(7) and H(8) resonances were calculated from the data using the value of K_d from the 4-CH_3 dilution data as an input parameter.

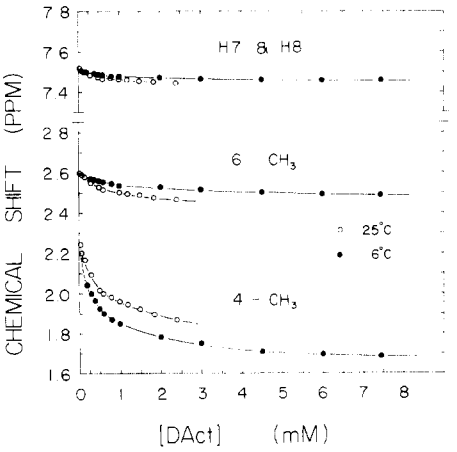

FIGURE 3: Concentration dependence of important groups of actinomycin D in D_2O–5 mM phosphate buffer (pD 7.4) at 6 and 25°C (no salt). The threonine methyl, sacrosine N-methyl, and methylvaline N-methyl resonances do not change much during the dilution and are not shown for clarity.

resonances; this is consistent with the formation of an inverted dimer (Figure 2)[2] because the benzenoid portion of the phenoxazone ring system has a much larger ring current than the quinoid portion of the phenoxazone ring. The interpretation of these induced shifts in the proton resonances in terms of a molecular geometry of the complex is well known (e.g., see Dwek, 1973 or Emsley et al., 1965).

A nonlinear least-squares program was used to calculate the limiting chemical shifts and the dimerization constant, K_d, assuming a simple dimerization

$$2A \overset{K_d}{\rightleftarrows} A_2 \tag{2}$$

for which the appropriate expression is

$$\delta_{obsd} - \delta_M = (\delta_D - \delta_M)\left(\frac{4K_d[A_0] + 1 - \sqrt{(8K_dA_0 + 1)}}{4K_dA_0}\right) \tag{3}$$

where δ_{obsd} is the observed chemical shift in the solution with a stoichiometric concentration A_0, δ_M is the chemical shift of the protons in the monomer state, and δ_D is the chemical shift of the protons in the dimer. The calculated values of the chemical shifts are listed in Table I and agree fairly well with the previously reported values. The values of the equilibrium constants are not in agreement with the previously reported values (Angerman et al., 1972) determined from ^1H NMR experiments because these authors used an incorrect expression[3] in relating the observed chemical shifts to the dimerization equilibrium. The equilibrium constants (Table I) calculated from the 4-CH_3 dilution data have a *calculated* standard deviation of ±15–20%. Thus the thermodynamic parameters calculated from the data in Table I will have a rather large uncertainty. The present dilution data were measured at 100 MHz and over the entire range of concentrations the 6-CH_3 group moved downfield a total of less than 12 Hz. These small changes in the chemical shifts (compared to the 35–40-Hz movement of the 4-CH_3) means that the 6-CH_3 and H(7) and H(8) data are much less reliable in terms of calculating values of the dimerization equilibrium constant. We have therefore used the value of K calculated from the 4-CH_3 data in order to calculate the values of δ_A and δ_{A_2} for the 6-CH_3 and H(7) and H(8) resonances (Table I). The dimerization constants will be of limited utility since the values of δ_{A_2} are temperature dependent, implying that the structure of the dimer is temperature dependent. The limiting chemical shifts of the 4-CH_3, 6-CH_3, and H(7) and H(8) proton resonances are independent of NaCl concentration.

Actinomycin D Complexes with the Deoxynucleotides Containing Guanine. The influence of the actinomycin D dimerization on the shape of the ^1H NMR titration curves is clearly illustrated in Figure 4 for the titration of actinomycin D with the self-complementary deoxydinucleotide pdG-dC. When the titration is performed at high concentrations of the drug (20 mM) the 4-CH_3 group moves downfield during the titration while the 6-CH_3 group moves upfield. If the effects of dimerization on the chemical shifts of the 4-CH_3 and the 6-CH_3 protons are taken into consideration, both the 4-CH_3 and the 6-CH_3 proton resonances of actinomycin D are shifted *upfield* as a result of complex formation between an actinomycin D monomer and the dinucleotide pdG-dC (Krugh and Neely, 1973b). This is clearly demonstrated in the low concentration actinomycin D titration with pdG-dC (Figure 4a) where the majority of the actinomycin D molecules (~80%) exist as monomers at the start of the titration. It is important to note that in the

[2] This figure is available in the microfilm edition of the journal.

[3] Equations 5 and 6 of Angerman et al. (1972) should be

$$\delta_{obsd} = X_A\delta_A + 2X_{A_2}\delta_{A_2}$$

and

$$\delta_{obsd} = \frac{[A_0] - 2[A_2]}{[A_0]}\delta_A + \frac{2[A_2]}{[A_0]}\delta_{A_2}$$

The form of the equations used by Angerman et al. (1972), although incorrect, did result in reasonable values for the infinite dilution chemical shifts. However, the equilibrium constants derived from their least-squares analysis are too large.

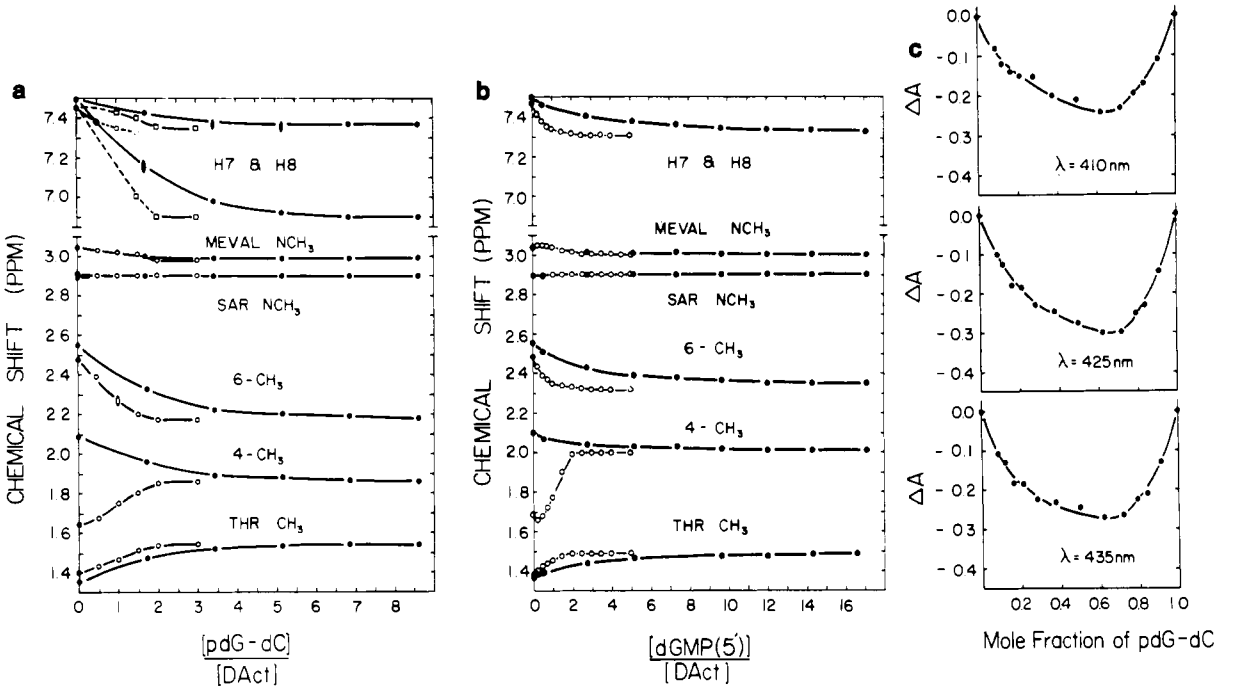

FIGURE 4: (a, left) Chemical shifts of selected actinomycin D groups plotted as a function of the nucleotide to drug ratio for pdG-dC at 6°C, 20 mM actinomycin D (○) and at 25°C, 0.34 mM actinomycin D (●). (b, center) Chemical shifts of selected actinomycin D groups plotted as a function of the nucleotide/drug ratio for dGMP (5′) at 6°C, 12 mM actinomycin D (○) and at 25 °C, 0.29 mM actinomycin D (●). (c, right) Continuous variation experiment for mixtures of pdG-dC and actinomycin D. The change in the absorbance (ΔA) at 410, 425, and 435 nm was measured at a constant total concentration of 4.2×10^{-4} M, while varying both the pdG-dC and actinomycin D concentrations.

presence of excess dinucleotide the chemical shifts of the actinomycin D protons are independent of the original concentration of the actinomycin D. Thus these chemical shifts are indicative of an actinomycin D–dinucleotide complex. The data in Figure 4b show the corresponding titrations of actinomycin D with dGMP where once again the titrations at both low (0.29 mM) and high (12 mM) concentrations of actinomycin D lead to the same conclusions if the dimerization of actinomycin D is taken into account. It is also important to consider the stoichiometry of complex formation before interpreting the induced chemical shifts in terms of a molecular geometry of the complex. In our earlier papers (Krugh, 1972; Krugh and Neely, 1973a,b) we presented evidence which supported the formation of a complex of actinomycin D with *two* guanine-containing nucleotides. A standard technique for determining the stoichiometry of complexes is the method of continuous variation (Job, 1928; Felsenfeld and Rich, 1957; Topal and Fresco, 1974) as illustrated for the formation of an actinomycin D complex with pdG-dC (Figure 4c). In this case the change in absorbance is used as a measure of the amount of complex formed. The data in Figure 4c show that the maximum amount of complex is formed at a mole fraction of pdG-dC $\simeq$ 0.6–0.7 consistent with the formation of a complex involving one actinomycin D and two pdG-dC molecules.

The deoxydinucleotides generally used in these studies (e.g., pdG-dC) have both an internal phosphate group (the 3′–5′ linkage) as well as a terminal 5′-phosphate group. The presence of the terminal phosphate is not expected to significantly influence the conformation of the complexes formed (Krugh, 1972) as shown by the fact that the chemical shifts of the 2:1 complex of dG-dC with actinomycin D are essentially the same as the chemical shifts of the 2:1 complex of pdG-dC with actinomycin (Figure 5).[2] The deoxydinucleoside monophosphates generally appear to have larger equi-

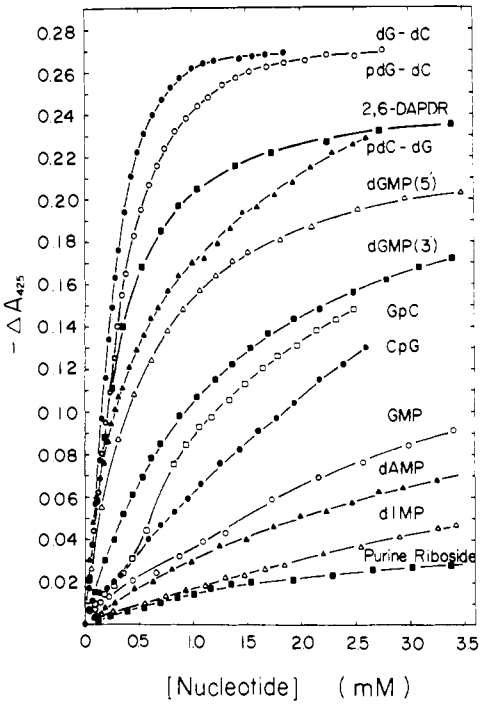

FIGURE 6: The change in the absorbance of actinomycin D at 425 nm. The concentration of actinomycin D was ~30 μM at the start of each titration. All measurements were made in 5 mM phosphate buffer (pH 7.0) and 25°C.

librium constants for the formation of drug–nucleic acid complexes. This phenomenon is illustrated in the visible spectral titrations of actinomycin D with pdG-dC and dG-dC shown in Figure 6. An analysis of the shape of the titration curves indicates that dG-dC binds stronger than pdG-dC.

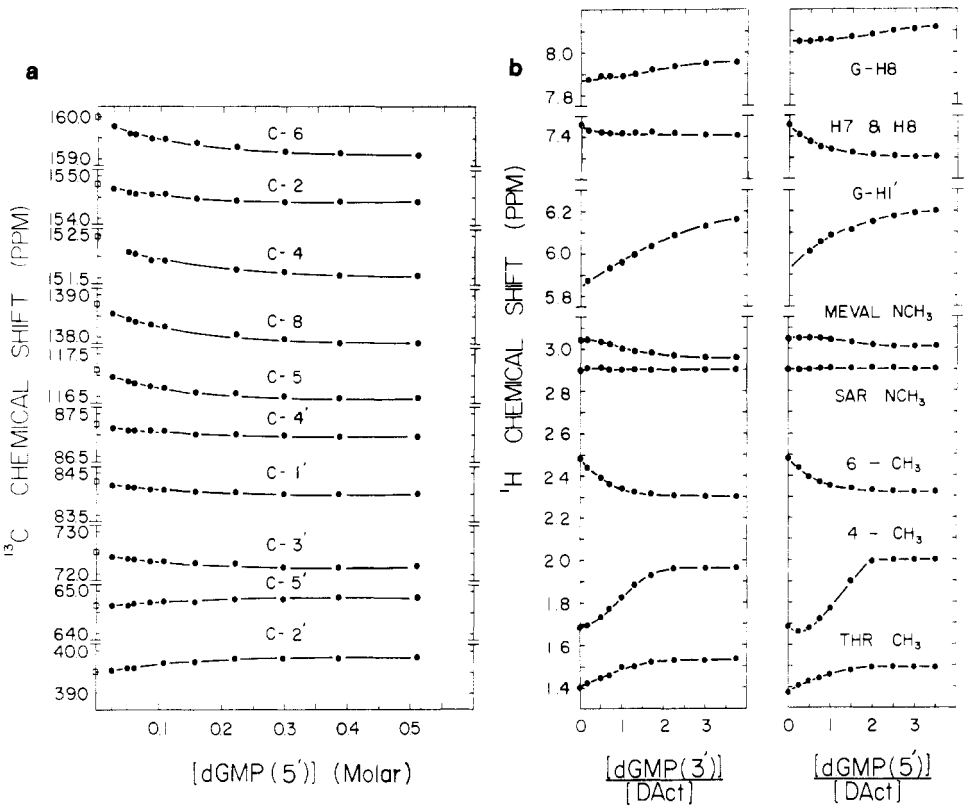

FIGURE 7: (a, left) Concentration dependence of the carbon-13 chemical shifts of deoxyguanosine 5′-monophosphate in D_2O at 30°C, pD 7.4. The infinite dilution shifts are indicated by the open squares. (b, right) Chemical shifts of selected actinomycin D groups and deoxyguanosine protons plotted as a function of the nucleotide to drug ratio for deoxyguanosine 3′-monophosphate and deoxyguanosine 5′-monophosphate at 6°C, 11.6 m*M* actinomycin D.

Table II: Induced Chemical Shifts of the Actinomycin D Protons that Result from Complex Formation with Selected Nucleotides

Nucleotide	$\Delta\delta$ (ppm)[a] 4-CH_3	6-CH_3	H(7) and H(8)
dG-dC	+0.44	+0.50	+0.66, 0.18
pdG-dC	+0.40	+0.47	+0.63, +0.16
5′-pdG (5′-dGMP)	+0.26	+0.33	+0.22
3′-pdG (3′-dGMP)	+0.30	+0.35	+0.12
pdC-dG	+0.34	+0.36	+0.27
5′-dIMP	(+0.39)[b]	(+0.32)[b]	(+0.13)[b]
2,6-DAPDR	+0.21	+0.27	+0.31

[a] A positive sign means that the given resonance moves upfield when an actinomycin D molecule (as a monomer) forms a complex with the nucleotide. We estimate that the uncertainties in these values are generally less than 0.05 ppm. [b] Estimated from the titration data in Figure 12, because the limiting chemical shift was not reached during the titration.

The induced chemical shifts of the actinomycin D protons that result from complex formation with pdG(5′-dGMP), pdG-dC, and dG-dC are listed in Table II and may be used to obtain information on the geometry of complex formation. The values for pdG and pdG-dC are slightly (but not significantly) different from our previously published values (Krugh and Neely, 1973a,b) because the recent availability of a Fourier transform NMR instrument has allowed us to determine more accurately the infinite dilution chemical shifts of the actinomycin D protons (Table I). The magnitudes of the induced shifts of the 4-CH_3, the 6-CH_3, and the H(7) and H(8) protons (Table II) are consistent with the formation of an actinomycin D-(pdG-dC)$_2$ complex in which the phenoxazone ring of actinomycin D is intercalated between the adjacent G·C base pairs of a miniature double helix. The induced chemical shifts of the actinomycin D-(pdG)$_2$ complex are consistent with a geometry of the complex in which the guanine rings are vertically stacked with the phenoxazone ring in essentially the same orientation as observed by Sobell et al. (1971) in the 1:2 actinomycin D-deoxyguanosine crystalline complex. Subsequent to our work, Patel (1974a,b) reported a nuclear magnetic resonance study of the actinomycin D complex with 5′-dGMP and pdG-dC. The ^{13}C NMR spectra of dGMP and a 1:2 actinomycin D solution with 5′-dGMP were recorded and the changes in the carbon-13 chemical shifts of the guanine base carbons were interpreted in terms of a geometry of complex formation. This procedure is only valid if the infinite dilution shifts of the guanine carbon resonances are known. Patel (1974a) estimated the infinite dilution chemical shifts from an investigation of the ^{13}C spectra of 5′-dGMP at 0.25 and 0.085 *M* concentrations. In view of the well-known aggregation of the nucleotides, it is inappropriate to extrapolate to infinite dilution from these relatively high concentrations of dGMP. To illustrate this point, and to provide further insight into the actinomycin D-(dGMP)$_2$ complex, we have measured the concentration dependence of the carbon-13 chemical shifts of 5′-dGMP over the concentration range of 0.025–0.5 *M* (Figure 7a). The lower concentrations required extensive time averaging (~17 hr) to record the spectra of the nonprotonated base carbons. The data in Figure 7a show the typical curvature in the plot of the chemical shift vs. concentration curves. Thus a linear extrapolation using any two points will incorrectly estimate the infinite dilution chemi-

Table III: ^{13}C Chemical Shifts and Induced Chemical Shifts of 5′-dGMP and the Actinomycin D–(5′-dGMP)$_2$ Complex.[a]

Guanosine Carbons	5′-dGMP		Act D–(5′-dGMP) Complex (Patel's Data, 0.063 M in D_2O, 30°)[d]	Δδ Induced Chemical Shifts[e]
	Patel's Data[b]	Our Infinite Dilution Shifts[c]		
C(6)	159.77	160.01	158.61	+1.40
C(2)	154.62	154.80	154.72	+0.08
C(4)	152.14	152.45	151.91	+0.54
C(8)	138.53	138.77	138.12	+0.65
C(5)	116.97	117.10	116.76	+0.34
C(4′)	87.02	87.22	88.23	−1.01
C(1′)	84.30	84.30	83.60	+0.70
C(3′)	72.38	72.51	73.30	−0.79
C(5′)	64.96	64.66	64.71	−0.05
C(2′)	34.62	39.47	39.76	−0.29

[a] The values given are in ppm downfield from Me_4Si. Dioxane was used as an internal reference and the listed values were calculated by using $\delta_{Me_4Si\text{-dioxane}} = 67.40$ ppm and $\delta_{Me_4Si-CS_2} = 193.7$ ppm. [b] D_2O solvent, pH ~7, 30° (Patel, 1974). These values are the estimated infinite dilution shifts from an investigation of the ^{13}C spectra at 0.25 and 0.085 M concentrations. Patel's data were converted to a Me_4Si scale. [c] These values were obtained by a graphical extrapolation of the data in Figure 9. [d] Patel, 1974. [e] These values represent the difference between the infinite dilution shifts (our data) and the chemical shifts of the carbons in the actinomycin D–(dGMP)$_2$ complex. A positive sign indicates that the resonance shifts upfield as a result of complex formation.

cal shifts. The magnitude and the sign of the errors will depend upon the magnitude and the sign of the induced chemical shifts that result from the formation of dimers or (*n*-mers). We have graphically estimated the infinite dilution ^{13}C chemical shifts from the data in Figure 7a using the concentration dependence of the G-H(8) and G-H(1′) proton chemical shifts as an additional guide. The data in Table III compare the infinite dilution chemical shifts for dGMP reported by Patel with the values determined from Figure 7a of this manuscript. We have also included in Table III the induced shifts, Δδ, for the formation of an actinomycin D–(dGMP)$_2$ complex.

The NMR data for a titration of actinomycin D with 3′-dGMP are shown in Figure 7b, along with a similar titration for 5′-dGMP. The 4-CH_3 and 6-CH_3 proton chemical shifts in the 3′-dGMP titration are invariant when the nucleotide/drug ratios are greater than 2:1, indicating the formation of a 2:1 complex. The H(7) and H(8) protons exhibit the only significant difference in the values of the induced chemical shifts for these two complexes. The H(7) and H(8) resonance is ~0.1 ppm more downfield in the actinomycin D–(3′-dGMP)$_2$ complex as compared to the actinomycin D–(5′-dGMP)$_2$ complex. This deshielding is consistent with the change in the location of the phosphate group, as will be discussed later. The sample of 3′-dGMP (P-L Biochemicals) was listed as 95 ± 5% pure. The downfield region of the ^1H NMR spectrum of this sample (Figure 8) shows that there are two base protons. The major peak at 8.003 ppm is from the G-H(8) proton of 3′-dGMP, while the small peak at 8.105 ppm is from the G-H(8) proton of 5′-dGMP. A consideration of the data in Figures 6, 7b, and 8 shows that the presence of the 15 ± 5% 5′-dGMP does not significantly affect the NMR results in Figure 7b. On the other hand, the NMR spectra provide both a sensitive means of determining nucleotide purity and the identification of the impurities.

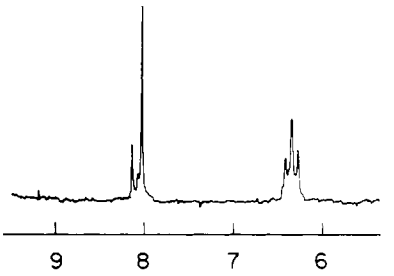

FIGURE 8: Downfield region of the 100-MHz proton spectrum of deoxyguanosine 3′-monophosphate at 25°C; 1 × 10^{-4} M EDTA was added to remove the line broadening caused by trace paramagnetic impurities.

Actinomycin D Complex with 5′-dIMP. The interaction of actinomycin D with 2′-deoxyinosine 5′-monophosphate (dIMP) was investigated in order to determine the effect of the purine 2-amino group on complex formation. Inosine lacks the 2-amino group of guanine, although both bases have a carbonyl group at the C(6) position. Poly(dI) binds actinomycin D even though it does not have the 2-amino group (Wells and Larson, 1970). The interaction between actinomycin D and dIMP was monitored by observing the changes in the visible spectrum (Figure 6) and the proton chemical shifts of actinomycin D (Figure 9a) that result from complex formation. The visible spectral titration indicates that dIMP forms only a weak complex with actinomycin D. A comparison of the chemical shift changes of the 4-CH_3 and 6-CH_3 groups during the dIMP and dGMP titrations indicates that dIMP binds to the 6-binding site of actinomycin D with a binding constant on the same order of magnitude as the 5′-dGMP binding ($K > 10^3$ M^{-1} at ~6°C) while dIMP binds to the 4-binding site with a much smaller binding constant than 5′-dGMP. These results should be compared to the visible spectral titration data where only the weak binding is observed. The implication is that the change in the visible spectrum of actinomycin D primarily monitors (and results from) the binding of nucleotides in the 4-binding site. The methylvaline N-CH_3 groups, which originally have the same chemical shift, titrate individually with dIMP (Figure 9a), which also indicates the presence of two binding sites with different binding constants. The induced chemical shifts of the 6:1 dIMP–actinomycin D solution show that complex formation results in the vertical stacking of the bases on the phenoxazone ring. This stacking is also reflected in the induced chemical shifts of the nucleotide protons. The I-H(2) and I-H(8) protons in the dIMP–Act D solutions are shifted upfield with respect to the infinite dilution shifts of dIMP. These upfield shifts also reflect the vertical stacking of the inosine and phenoxazone rings. As the dIMP/Act D ratio is increased the chemical shifts of the I-H(2) and I-H(8) protons gradually move toward the free inosine values, reflecting the fast chemical exchange (on the NMR time scale) between free and bound nucleotides. The chemical shifts of the inosine protons, when extrapolated to the 0:1 ratio of dIMP/Act D, provide a measure of the chemical shifts of the inosine protons in the dIMP–Act D complex. However, as a result of the two different types of binding, the induced chemical shifts ($\Delta\delta$(I-H(2)) = 0.20 ppm; $\Delta\delta$(I-H(1′)) = 0.37 ppm) that are calculated from this approach must be carefully interpreted because the observed values will be a weighted average of the induced shifts in the two sites.

Actinomycin D Complexes with 2,6-Diaminopurine Deoxyribose (2,6-DAPDR) and 5′-dAMP. The visible spec-

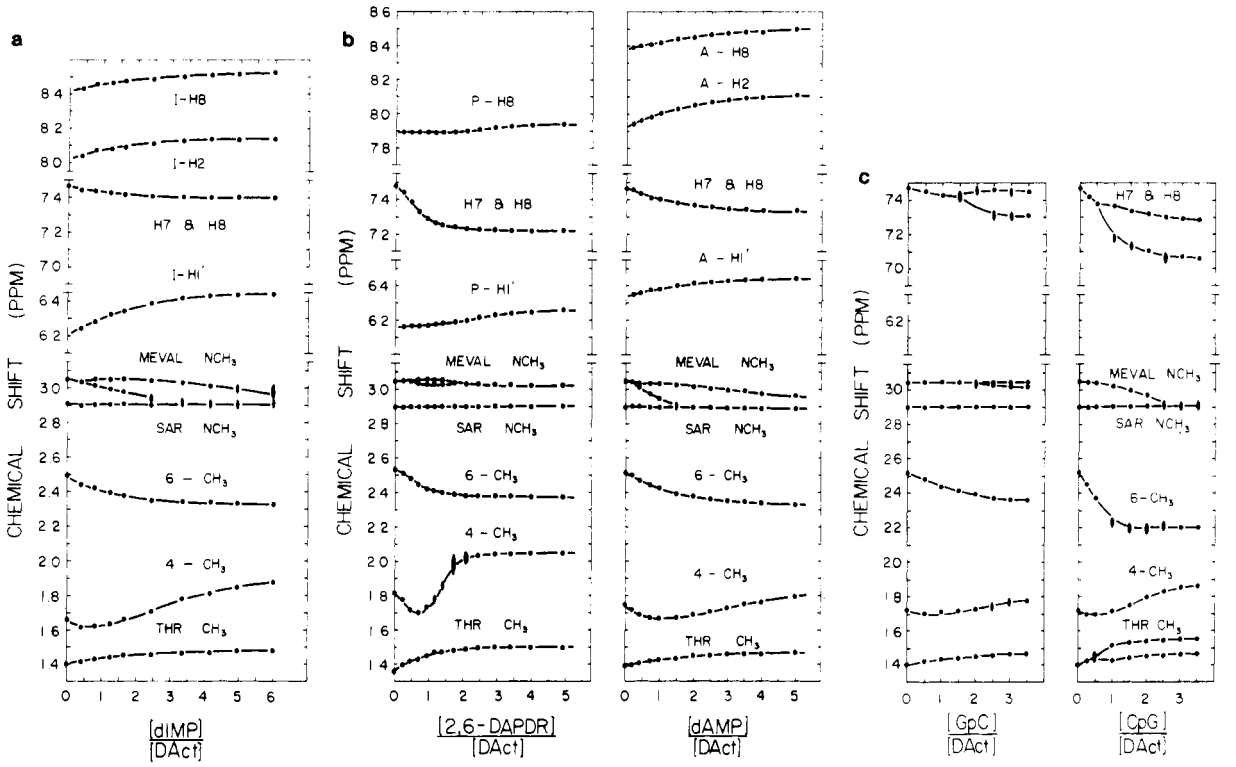

FIGURE 9: (a, left panel) Chemical shifts of selected actinomycin D groups and deoxyinosine 5′-monophosphate protons plotted as a function of the nucleotide/drug ratio at 6°C and 10.6 m*M* actinomycin D. (b, middle two panels) Chemical shifts of selected actinomycin D groups and nucleotide groups plotted as a function of the nucleotide/drug ratio for 2,6-diaminopurine-2′-deoxyribose at 6°C (1.47 m*M* actinomycin D) and for deoxyadenosine 5′-monophosphate at 6°C (2.99 m*M* actinomycin D). (c, right panels) Chemical shifts of selected actinomycin D groups plotted as a function of the nucleotide/drug ratio for G-C and C-G at 6°C, 4.34 m*M* actinomycin D.

tral titration of actinomycin D with 2,6-diaminopurine 2′-deoxyribose (Figure 6) shows that this compound binds to actinomycin D even stronger than 5′-dGMP. The NMR titration of actinomycin D with 2,6-diaminopurine deoxyribose (Figure 9b) also shows clear evidence that actinomycin D will bind two of the 2,6-DAPDR molecules and that this nucleotide binds strongly to both the 4- and 6-binding sites. The two methylvaline N-CH_3 groups exhibit slightly different chemical shifts during a portion of the titration. This observation, along with the initial upfield shift of the 4-CH_3 group, is consistent with the 2,6-diaminopurine deoxyribose binding to the actinomycin D dimer during the earlier parts of the titration. The methylvaline N-CH_3 groups become equivalent again after the majority of the dimers are disrupted by the binding of the nucleotide. The induced upfield shifts that result from complex formation (Table II) clearly show that the two 2,6-diaminopurine dexoyribose molecules are stacked on the phenoxazone ring. The magnitude of these induced shifts suggests that the orientation of the purine rings is quite similar to the orientation of the guanine ring in the actinomycin D-$(dGMP)_2$ complex.

A comparison of the titration data for deoxyadenosine 5′-monophosphate (dAMP) with 2,6-diaminopurine deoxyribose in both the visible and NMR spectral titrations (Figures 6 and 9b) shows the clear difference in the binding of these two deoxynucleotides. The NMR spectra show that dAMP binds much weaker to the 4-binding site than to the 6-binding site (see also Krugh and Neely, 1973a). Note, for example, the different titration behavior of the methylvaline N-CH_3 groups. Once again the data indicate that the visible spectral titrations primarily monitor the nucleotide binding at the 4-binding site of actinomycin D.

G-C and C-G Complexes with Actinomycin D. The complex formation between actinomycin D and the self-complementary ribodinucleoside monophosphates G-C and C-G has also been monitored by observing the changes in the visible spectra and the proton magnetic resonance spectra of actinomycin D (Figures 6 and 9c). A comparison of the G-C and dG-dC titration curves in both the visible (Figure 6) and proton magnetic resonance spectra (Figures 5 and 9c) dramatically shows that the presence of the 2′-hydroxy group reduces the binding affinity (primarily as a result of the steric and electrostatic repulsion between the 2′-hydroxyl group and the phenoxazone ring 2-amino and 3-carbonyl groups). This is consistent with the well-known fact that actinomycin D does not bind to double-stranded RNA. The C-G ^1H NMR titration (Figure 9c) looks similar to the titration of actinomycin D with GMP (Figure 4 of Krugh and Neely, 1973a). Because of the reduced binding affinity of these ribodinucleoside monophosphates the data do not provide much detailed geometrical information, except that the G-C and C-G molecules form stacked complexes with actinomycin D.

Actinomycin D–Purine Ribose Complex Formation. The interaction of actinomycin D with purine ribose was monitored by both absorbance and proton magnetic resonance spectroscopy. The ΔA vs. nucleoside concentration data (Figure 6) indicate only a very weak complex formation. The ^1H NMR experiments on the other hand (Figure 10)[2] are rather interesting in that the trend in the chemical shifts as a function of the purine ribose/actinomycin D ratio indicate that the purine ribose has a very small binding constant for the 4-binding site and a much larger binding constant for the 6-binding site (although weaker than dGMP). For example, note that the chemical shift of one of the methylvaline N-CH_3 groups is unchanged during the titration

while the other one moves upfield as usual. The 6-CH_3 group and the H(7) and H(8) protons provide clear evidence of complex formation, while the chemical shift of the 4-CH_3 is relatively constant throughout the titration. These data suggest that the purine ribose does not destack the actinomycin D dimers that are present at the high concentration (0.013 *M*) of actinomycin D used for these experiments. As discussed previously (Krugh and Neely, 1973a), it is possible for the nucleotide to bind to the actinomycin D dimer.

2-Chloroadenosine Complex with Actinomycin D. The ^1H NMR data for the titration of actinomycin D with 2-chloroadenosine are shown in Figure 11.[2] The chemical shifts of all the protons reflect the vertical stacking of the purine base with the phenoxazone ring. The shape of the 4-CH_3, 6-CH_3, and the two separate curves for the methylvaline N-CH_3 groups suggest that there are two binding sites with different binding constants.

Discussion

Actinomycin D Dimerization. The present experiments provide reliable values for the actinomycin D chemical shifts in both the monomer, δ_A, and dimer, δ_{A_2}, form. It is reassuring to observe that, within experimental error, the chemical shifts of the 4-CH_3, the 6-CH_3, and the H(7) and H(8) resonances of the actinomycin D monomer are independent of temperature and ionic strength (Table I). The chemical shifts of the dimer are independent of ionic strength but, on the other hand, they are a function of temperature. Note that δ_{A_2} (4-CH_3) shifts 10 Hz *downfield* as the temperature goes from 6 to 25°C while δ_{A_2} (6-CH_3) shifts *upfield* 9 Hz. This observation is consistent with the formation of an inverted dimer in which the temperature dependence of the chemical shifts results from a small change in the structure of the dimer, such as a lateral movement of the phenoxazone rings with respect to one another (e.g., see Angerman et al., 1972). As a result, the thermodynamic parameters derived from these measurements are not strictly valid. Although proton magnetic resonance measurements probably provide the most sensitive means of determining the dimerization constant (compare, for example, the small scatter in the points shown in Figure 3 with the equilibrium centrifugation results of Crothers et al., 1968) there is still a 15–20% uncertainty in the equilibrium constant calculated from the 4-CH_3 dilution data. A more precise determination of the equilibrium constants would require the measurement of the dilution data on a Fourier transform high frequency (e.g., 270 MHz) NMR instrument where the increased sensitivity and resolution would simplify the experiments.

The Influence of Self-Association on the Observed Chemical Shift Changes. Before interpreting the observed changes in the chemical shifts that result from the formation of a complex it is important that the effects of dimerization of the reactants be carefully considered. The formation of a complex of actinomycin D with 5′-dGMP serves as an excellent example of this point. In the first application of NMR to investigate a 1:1 complex of actinomycin D with 5′-dGMP, Danyluk and Victor (1970) observed that as a result of complex formation the 6-CH_3 and the H(7) and H(8) proton resonances moved upfield while the 4-CH_3 proton resonance moved downfield *with respect to the spectrum of actinomycin D under the same experimental conditions.* From these results they proposed a structure in which the guanine ring was stacked over the benzenoid portion of the phenoxazone ring while the ribose and phosphate groups were in the vicinity of the 4-CH_3 group. This geometry would account for the apparent deshielding of the 4-CH_3 group, while at the same time accounting for the upfield shifts of the 6-CH_3 and H(7) and H(8) protons. This proposed geometry is of course incorrect because in these initial experiments Danyluk and Victor (1970) failed to consider the effect of actinomycin D dimerization on the chemical shifts of the phenoxazone ring protons. The data in Figure 4 clearly demonstrate that the chemical shift changes observed *during the course of a titration* depend upon the initial concentration of the actinomycin D. It is equally important to note that the actinomycin D chemical shifts that are observed in the presence of excess 5′-dGMP, pdG-dC, or other dinucleotides containing guanine are *independent* of the initial actinomycin D concentration. As we previously explained (Krugh and Neely, 1973a,b) and conclusively demonstrate in Figure 4 the overall net downfield shift of the 4-CH_3 group during the high concentration [>1 m*M*] actinomycin D titrations with nucleotides containing guanine actually results from a large downfield shift due to a destacking of the actinomycin D dimers (~0.7 ppm) partially offset by an induced upfield shift (0.3–0.4 ppm) that results from the formation of an actinomycin D complex with the guanine base of the nucleotides. We thus feel confident in interpreting the induced proton chemical shifts that result from complex formation in terms of a molecular geometry of the complex.

It should be obvious that the stoichiometry of the complex is an equally important consideration. The actinomycin D-dGMP titration again serves as a useful model to illustrate this point because it should be clear that the geometry of the complex that would have to be proposed in order to account for the observed chemical shift changes would be different if the stoichiometry of the complex were assumed to be 1:1 as opposed to the actual 2:1 dGMP-actinomycin D complexes. The 2:1 nucleotide-actinomycin D stoichiometry of the complexes is obvious from the high concentration actinomycin D titrations with the guanine containing nucleotides where the chemical shifts of the actinomycin D phenoxazone ring protons cease changing at a 2:1 nucleotide-actinomycin D ratio (see also Krugh and Neely, 1973a,b; Arison and Hoogsteen, 1970). It is interesting to compare this result with the visible spectral titration of actinomycin D with 5′-dGMP where the hyperbolic binding curve had led previously workers to assume that a 1:1 complex was formed (e.g., Kersten, 1961; Reich, 1964; Gellert et al., 1965; Behme and Cordes, 1965). The presence of two independent binding sites with similar binding constants would also produce a nearly hyperbolic binding curve and this appears to be the case when actinomycin D forms a complex with 5′-dGMP. The sigmoidal shape of the visible spectral titration curves of actinomycin D with pdG-dC (Figure 6, and Krugh, 1972) and dG-dC (Figure 6) clearly show that actinomycin D forms a complex with more than one dinucleotide. The 2:1 dinucleotide-actinomycin D stoichiometry of complex formation is indicated by both the ^1H NMR titrations (Krugh, 1973b) and the method of continuous variation (Figure 4c).

The induced chemical shifts of the nucleotide protons or carbon-13 nuclei may also be used to monitor complex formation with the hope of providing corroborating evidence on the geometry of the complex. Since it is well known that in aqueous solutions the mononucleotides tend to self-associate by vertical stacking of the bases (e.g., see Jardetzky,

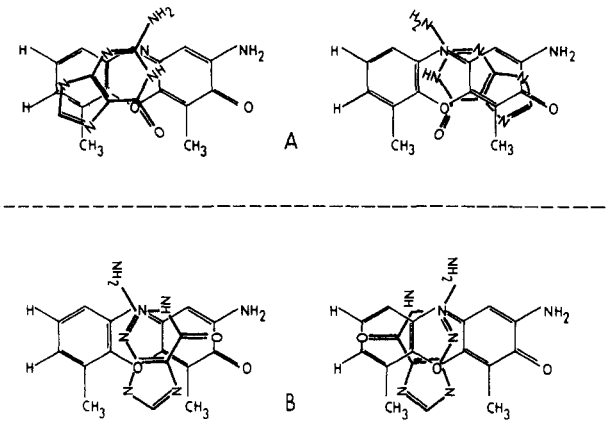

FIGURE 12: (A) Stacking patterns observed in the crystal structure of actinomycin D and deoxyguanosine (Jain and Sobell, 1972). It should be noted that these structures represent projections of the guanine ring onto the phenoxazone ring and thus the apparent overlap of the rings will depend upon the projection plane. (B) The alternative geometries of the complex as proposed by Patel (1974a).

1964; Schweizer et al., 1965, and Ts'o et al., 1969) it is important to determine the infinite dilution chemical shifts of the nucleotides in order to provide the correct reference state for determining the induced chemical shifts that result from complex formation. The infinite dilution chemical shifts of 5′-dGMP are listed in Table III, along with the recently published values of Patel (1974a) that were determined by a two point extrapolation (0.25 and 0.085 *M*) to infinite dilution. These two sets of infinite dilution chemical shifts differ by no more than 0.3 ppm, but a discrepancy of this magnitude is very important if the induced shifts that result from complex formation are to be interpreted in terms of a molecular geometry. If we use the data in Figure 7a and *linearly* extrapolate our data to infinite dilution from the 0.25 and 0.085 *M* points we obtain values that are essentially the same (within experimental error) as the values reported by Patel (1974a). Using the ^{13}C chemical shifts of the actinomycin D–$(dGMP)_2$ complex measured by Patel (1974a) and our data for the infinite dilution shifts of dGMP, we may calculate a revised set of induced shifts for the nucleotide carbons ($\Delta\delta$ in Table III) that result from complex formation. We note that the G-C(6) carbon is shifted upfield +1.4 ppm as a result of complex formation, while the G-C(2) carbon resonance is upfield shifted only +0.08 ppm. Patel proposed alternative stacking geometries (Figure 12) from that determined in the solid state (Jain and Sobell, 1972) and in solution (Krugh and Neely, 1973a) to account for the unusually large upfield shift (+1.4 ppm) of the guanine-C(6) carbon. However, even if *all* of the guanine bases were oriented so that the C(6) carbon atoms were stacked 3.4 Å above or below the *benzenoid* portion of the chromophore (where the ring current of the phenoxazone ring is at a maximum) we would expect to observe an upfield shift of only ~1.2 ppm, if we use the isoshielding curves for the phenoxazone ring presented by Patel (1974a) to predict the induced shifts of the guanine carbons. Even more important is the fact that the guanine C(2) carbon resonance is upfield shifted less than 0.1 ppm as a result of complex formation. The guanine C(5) carbon is upfield shifted +0.34 ppm, while the C(4) carbon is upfield shifted +0.54 ppm as a result of complex formation. We find it impossible to propose a geometry (or combination of geometries) in which the guanine rings may be stacked on the actinomycin D phenoxazone ring in order to simultaneously account for the observed induced shifts in all of the guanine carbons. For example, using the isoshielding curves for the phenoxazone ring proposed by either Patel (1974a) or Angerman et al. (1972) we would expect to observe at least a +0.5 ppm upfield shift of the guanine C(2) carbon for virtually any combination of the geometries shown in Figure 12. We therefore conclude that the induced shifts in the guanine carbon-13 resonances arise from several sources. Changes in the geometric or electronic structure of guanine, as well as "solvent effects" or "medium effects" (e.g., Stothers, 1972; Levy and Nelson, 1972) that result from complex formation must be partly responsible for the changes in the chemical shifts of the carbon resonances that are observed when a complex is formed. This is unfortunate because the carbon-13 data would be very helpful in determining the geometry of the complexes *if* the observed chemical shift changes were a result of only ring current induced shifts. There has been very little work done on the quantitative use of ring current shifts of carbon-13 nuclei to determine geometries of complexes and in the actinomycin D–dGMP system it is apparently inappropriate to interpret the chemical shift changes in terms of only ring current shifts. This conclusion is buttressed by any attempt to reconcile the induced shifts observed in the proton NMR spectra with those observed in the carbon-13 spectra. Thus there is no solid evidence in either the carbon-13 or proton magnetic resonance data to support the alternative binding schemes proposed by Patel (1974a). This does not exclude the possibility that a *small fraction* of the complexes exist in these (or other) alternative binding schemes because the NMR data in the present fast chemical exchange limit provide information on the weighted ensemble average of all the complexes present in solution.

Actinomycin D Complexes with pdG-dC and dG-dC. The formation of an actinomycin D complex with *two* pdG-dC (or dG-dC) dinucleotides is shown by both the ^1H NMR results and the visible spectral titrations. The induced chemical shifts of the 4-CH_3 (~0.40 ppm) and the 6-CH_3 (~0.47 ppm) groups are consistent with the formation of a complex in which the phenoxazone ring is intercalated between two G·C base pairs to form a miniature double helical complex. It is worth noting that the induced shifts of the 4-CH_3 and 6-CH_3 groups in the actinomycin D–$(dGMP)_2$ complex (0.26 and 0.33 ppm, respectively) are consistent with the formation of a complex in which the guanine bases are oriented with respect to the phenoxazone ring in exactly the same manner as in the actinomycin D–$(pdG\text{-}dC)_2$ complex, since the shielding of the cytosine base would account for the additional 0.14-ppm upfield shift of both the 4-CH_3 and 6-CH_3 groups observed in the actinomycin D–$(pdG\text{-}dC)_2$ complex when compared to the chemical shifts of these groups in the actinomycin D–$(5'dGMP)_2$ complex. We consider this as another indication that the geometry of the complex of actinomycin D with 5′-dGMP in solution is very similar to that observed in the solid state. The splitting of the H(7) and H(8) protons into the well-resolved AB pattern in the actinomycin D–$(pdG\text{-}dC)_2$ complex is consistent with the phosphodiester bridge being located in the vicinity of the H(7) and H(8) protons since the magnetic anisotropy of the phosphate group can satisfactorily account for this splitting.

The interpretation of the induced proton chemical shifts in terms of a geometry of the complex suffers from the same general limitations as the carbon-13 data. However, the magnitudes of the "solvent effects" or "medium effects"

are expected to be much smaller in the proton spectra as compared to the carbon-13 spectra. When $\Delta\delta \geq 0.2$ ppm the main limitation in the use of proton spectroscopy to deduce the geometries of the complexes appears to be the accuracy of the theoretically calculated isoshielding curves. In the present case we are fortunately able to compare the observed induced shifts ($\Delta\delta$) with those predicted from the geometry of Sobell and Jain (1972). As stated above, and before (Krugh and Neeley, 1973a,b; Krugh, 1974), we conclude that the solution geometries are very similar to that observed or predicted on the basis of the cocrystalline complex of actinomycin D with deoxyguanosine.

Actinomycin D Complex with Deoxyguanosine 3′-Monophosphate (3′-dGMP). The ^{1}H NMR data for the titration of actinomycin D with deoxyguanosine 3′-monophosphate (Figure 7b) are consistent with the formation of a complex in which two guanine bases are stacked on the phenoxazone ring in essentially the same orientations as in the actinomycin D complex with 5′-dGMP. The few hertz difference in the induced shifts of the 4-CH_3 and 6-CH_3 groups in the actinomycin D–(3′-dGMP)$_2$ complex when compared to the actinomycin D–(5′-dGMP)$_2$ complex (Table I) are not very significant. The H(7) and H(8) protons remain a singlet and are shifted upfield approximately 8–9 Hz less in the 3′-dGMP complex with actinomycin D. In view of the splitting of the H(7) and H(8) protons into an AB pattern for the complex of actinomycin D with pdG-dC (Figure 4a), as well as complexes of actinomycin D with pdG-dT, and pdG-dA (Krugh and Neely, 1973b), we had anticipated that the 3′-phosphate group of 3′-dGMP would also result in the observation of an AB pattern for the H(7) and H(8) protons. However, the location of the 3′-phosphate group in the actinomycin D complex with 3′-dGMP is much less restricted than in the case of the sandwich type of complex formed when actinomycin D complexes with pdG-dC, pdG-dT, or pdG-dA where the phosphate group under discussion serves as the 3′–5′ phosphodiester bridge. The conformation of the 3′-phosphate group of 3′-dGMP which results in the formation of a hydrogen bond between the 5′-hydroxyl proton and one of the phosphate oxygens also provides maximum exposure of the phosphate group to the solvent water molecules in the actinomycin D–(3′-dGMP)$_2$ complex and concurrently minimizes the interaction between the phosphate group and the hydrophobic phenoxazone ring.

Actinomycin D Complex with G-C and C-G. Both the visible spectral data (Figure 6) and the ^{1}H NMR data (Figure 9c) show the remarkable difference in the titration of actinomycin D with G-C when compared to the deoxy compound dG-dC. The much reduced binding affinity of G-C is consistent with the well-known fact that actinomycin D does not bind to double-stranded RNA. This selectivity is easily understood in terms of the geometry of the intercalated complex where the presence of the 2′-hydroxyl group would result in unfavorable steric and electrostatic interactions (e.g., see Sobell and Jain, 1972). The dinucleoside monophosphates have a great deal more flexibility than double-stranded RNA and it is reassuring to see that our simple model compounds reflect the binding preferences that actinomycin D exhibits with polynucleotides. In this regard we note that in our ethidium bromide studies (Krugh, 1974; Krugh et al., 1975b; Krugh and Reinhardt, 1975) we found that ethidium formed intercalative complexes with complementary mixtures of both the deoxy- and ribodinucleotides, which is consistent with the observation that ethidium intercalates into both double-stranded DNA and RNA.

General Comments. It is quite interesting to compare the binding data for 5′-dGMP, 5′-dAMP, 5′-dIMP, and 2,6-diaminopurine deoxyribose. We previously noted (Krugh and Neely, 1973a,b) that dGMP binds strongly to both the 4- and the 6-binding sites, while dAMP preferentially binds to the 6-binding site. This preferential binding is also observed for dIMP, while 2,6-diaminopurine deoxyribose binds strongly to both binding sites. An initial consideration of the structures of these nucleotides suggests that only the nucleotides with a 2-amino group exhibit strong binding in the 4-binding site, while all of these nucleotides appear to bind strongly at the 6-binding site. One interpretation of these observations is that the 2-amino group participates in hydrogen bond formation which is important in stabilizing the complex. In the actinomycin D–deoxyguanosine crystal structure the 2-amino group of deoxyguanosine formed a hydrogen bond with the L-threonine carbonyl group of the cyclic pentapeptide in *both the 4- and the 6-binding sites.* Sobell and coworkers (e.g., Sobell and Jain, 1972) proposed that this hydrogen bond formation was the source of the general requirement for guanine when the drug binds to DNA. However, since *both* of the deoxyguanosine 2-amino groups formed a strong hydrogen bond with the carbonyl groups of the L-threonines, we would expect that the loss of the hydrogen bond in going from the dGMP to the dIMP complex should have an approximately identical effect on the nucleotide binding in *both* the 4- and the 6-binding sites. We do not observe this to be the case and we thus conclude that stacking forces are also important in stabilizing both the actinomycin D–nucleotide complexes, and, by analogy, the actinomycin D–DNA complex. The importance of the stacking forces was clearly illustrated in the fact that actinomycin D is able to orient the bases of the deoxydinucleotides when a complex is formed (e.g., Krugh, 1972; Krugh and Neely, 1973a,b). The importance of the stacking forces clearly leads to the conclusion that the drug will preferentially bind to certain sequences available as intercalation sites since the nature of a helix results in sequence dependent stacking patterns. In separate experiments involving the complex formation of actinomycin D with complementary mixtures of mono- and dinucleotides (Krugh, 1974; and unpublished results) we have obtained independent evidence that when actinomycin D binds to DNA, the general requirement for guanine appears to be a result of the electronic structure of the 4-binding site. However, we will postpone further discussion of the exciting biological implications of these observations until these additional experiments are presented in detail.

Supplementary Material Available

Figures 2, 5, 10, and 11 will appear following these pages in the microfilm edition of this volume of the journal. Photocopies of the supplementary material from this paper only or microfiche (105 × 148 mm, 24× reduction, negatives) containing all of the supplementary material for the papers in this issue may be obtained from the Business Office, Books and Journals Division, American Chemical Society, 1155 16th St., N.W., Washington, D.C. 20036. Remit check or money order for $4.00 for photocopy or $2.50 for microfiche, referring to code number Bio-75-4912.

References

Angerman, N. S., Victor, T. A., Bell, C. L., and Danyluk, S. S. (1972), *Biochemistry 11,* 2402.

Arison, B. H., and Hoogsteen, K. (1970), *Biochemistry 9,* 3976.
Behme, M. T. A., and Cordes, E. H. (1965), *Biochim. Biophys. Acta 108,* 312.
Benz, F. W., Feeney, J., and Roberts, G. C. K. (1972), *J. Magn. Reson. 8,* 114.
Crothers, D. M., Sabol, S. L., Ratner, D. I., and Müller, W. (1968), *Biochemistry 7,* 1817.
Danyluk, S. S., and Victor, T. A. (1970), *Jerusalem Symp. Quantum Chem. Biochem. 2,* 394.
Dwek, R. A. (1973), Nuclear Magnetic Resonance in Biochemistry, London, Oxford University Press, pp 48–61.
Emsley, J. W., Feeney, J., and Sutcliffe, L. H. (1965), High Resolution Nuclear Magnetic Resonance Spectroscopy, New York, N.Y., Pergamon Press.
Felsenfeld, G., and Rich, A. (1957), *Biochim. Biophys. Acta 26,* 457.
Gellert, M., Smith, C. E., Neville, D., and Felsenfeld, G. (1965), *J. Mol. Biol. 11,* 445.
Goldberg, I. H., and Friedman, P. A. (1971), *Annu. Rev. Biochem. 40,* 775.
Jain, S. C., and Sobell, H. M. (1972), *J. Mol. Biol. 68,* 1.
Jardetzky, O. (1964), *Biopolym. Symp. 1,* 501.
Job, P. (1928), *Ann. Chim. 9,* 113.
Kersten, W. (1961), *Biochim. Biophys. Acta 47,* 610.
Kersten, W., Kersten, H., and Rauen, H. M. (1960), *Nature (London) 187,* 60.
Kirk, J. M. (1960), *Biochim. Biophys. Acta 42,* 167.
Krugh, T. R. (1972), *Proc. Natl. Acad. Sci. U.S.A. 69,* 1911.
Krugh, T. R. (1974), Molecular and Quantum Pharmacology, Bergmann, E., and Pulman, B., Ed., Dordrecht, Holland, Reidel Publishing Co., *7,* 465.
Krugh, T. R., Laing, J. W., and Young, M. A. (1975a), submitted for publication.
Krugh, T. R., and Neely, J. W. (1973a), *Biochemistry 12,* 1775.
Krugh, T. R., and Neely, J. W. (1973b), *Biochemistry 12,* 4418.
Krugh, T. R., and Reinhardt, C. G. (1975), *J. Mol. Biol.* (in press).
Krugh, T. R., Wittlin, F. N., and Cramer, S. P. (1975b), *Biopolymers 14,* 197.
Krugh, T. R., and Young, M. A. (1975), *Biochem. Biophys. Res. Commun. 62,* 1025.
Levy, G. C., and Cargioli, J. D. (1972), *J. Magn. Reson. 6,* 143.
Levy, G C., and Nelson, G. L. (1972), Carbon-13 Nuclear Magnetic Resonance for Organic Chemists, New York, N.Y., Wiley.
Mooberry, E. S., and Krugh, T. R. (1975), *J. Magn. Reson. 17,* 128.
Patel, D. J. (1974a), *Biochemistry 13,* 1476.
Patel, D. J. (1974b), *Biochemistry 13,* 2388.
Patt, S. L., and Sykes, B. D. (1972), *J. Chem. Phys. 56,* 3182.
Reich, E. (1964), *Science 143,* 684.
Reich, E., and Goldberg, I. H. (1965), *Prog. Nucl. Acid. Res. 3,* 183.
Schweizer, M. P., Chan, S. I., and Ts'o, P. O. P. (1965), *J. Am. Chem. Soc. 87,* 5241.
Smith, M. (1963), *Biochem. Biophys. Res. Commun. 10,* 67.
Sobell, H. M. (1973), *Prog. Nucl. Acid Res. 13,* 153.
Sobell, H. M., and Jain, S. C. (1972), *J. Mol. Biol. 68,* 21.
Sobell, H. M., Jain, S. C., Sakore, T. D., and Nordman, C. E. (1971), *Nature (London) 231,* 200.
Stothers, J. B. (1972), Carbon-13 NMR Spectroscopy, New York, N.Y., Academic Press.
Topal, M. D., and Fresco, J. R. (1974), *Biophys. Chem. 2,* 193.
Tsai, C. C., Jain, S. C., and Sobell, H. M. (1975), *Proc. Natl. Acad. Sci. U.S.A. 72,* 628.
Ts'o, P. O. P., Kondo, N. S., Schweizer, M. P., and Hollis, D. P. (1969), *Biochemistry 8,* 997.
Van Geet, A. L. (1970), *Anal. Chem. 42,* 679.
Wells, R. D., and Larson, J. E. (1970), *J. Mol. Biol. 49,* 319.
Young, M. A., and Krugh, T. R. (1975), *Biochemistry* (in press).